ARTICLE OPEN ACCESS

Clinical Pharmacology Overview of Tislelizumab in Patients With Advanced Tumors With a Focus on Racial Impact

Tian Yu[1] (ID) | Chi-Yuan Wu[1] | Srikumar Sahasranaman[1] | Xianbin Tian[2] | Ying Fei Li[3] | Zhiyu Tang[1] | Yanfei Yang[4] | Ya Wan[5] | Quting Zhang[5] | Patrick Schnell[6] | Ariadna Mendoza-Naranjo[7] | Ramil Abdrashitov[8] | William D. Hanley[1] | Nageshwar Budha[1] (ID)

[1]Clinical Pharmacology and Pharmacometrics, BeiGene USA, Inc., San Carlos, California, USA | [2]PK Sciences, Novartis Biomedical Research, Novartis Pharmaceutical, Inc., East Hanover, New Jersey, USA | [3]Pharmacometrics, Oncology, Global Drug Development, Novartis Pharmaceutical, Inc., East Hanover, New Jersey, USA | [4]Clinical BA BeiGene (Shanghai) Co., Ltd., Shanghai, China | [5]Scientific Programming, BeiGene (Shanghai) Co., Ltd., Shanghai, China | [6]Global Product Safety, BeiGene USA, Inc., Ridgefield Park, New Jersey, USA | [7]Clinical Development, BeiGene UK, Ltd., London, UK | [8]Clinical Development, BeiGene USA, Inc., Fulton, Maryland, USA

Correspondence: Nageshwar Budha (nageshwar.budha@beigene.com)

ABSTRACT

Tislelizumab, an anti-programmed cell death protein-1 monoclonal antibody, has demonstrated improved survival over the standard of care for multiple cancers. However, tislelizumab's effectiveness across different racial/ethnicity groups warrants further evaluation. This clinical pharmacology overview includes tislelizumab's pharmacokinetic properties, correlations with efficacy and safety, and immunogenicity, with a focus on racial impact. Non-compartmental pharmacokinetic analysis was conducted using data from Asian and White patients enrolled in BGB-A317-001 and BGB-A317-102. Population pharmacokinetic analyses used pooled data from 12 clinical studies to evaluate the impact of intrinsic/extrinsic factors on tislelizumab's pharmacokinetic properties, including race effect. Exposure–efficacy/exposure–safety relationships and immunogenicity assessments were evaluated for the phase III BGB-A317-302/-303 studies. Tislelizumab exhibited dose-proportional pharmacokinetics, and there were no clinically meaningful differences in tislelizumab's pharmacokinetic parameters at 200 mg once every 3 weeks between BGB-A317-001 ($n = 12$, 83% White patients) and BGB-A317-102 ($n = 20$, 100% Chinese patients); race was not a significant covariate. No clinically relevant exposure–efficacy/−safety relationships were observed in BGB-A317-302/-303. Incidence of anti-drug antibodies (ADAs) was similar between Asian and White patients. The presence of ADAs was not clinically relevant for tislelizumab's pharmacokinetic properties, efficacy, or safety. There were no differences in tislelizumab's pharmacokinetic or ADA characteristics between Asian and White patients with advanced cancer and no clinically relevant exposure–efficacy/−safety dependency or impact of immunogenicity on efficacy and safety. Data from the extensive clinical program of tislelizumab support the use of tislelizumab across broad patient populations with relevant tumor types.

Summary

- What is the current knowledge on the topic?
  - Tislelizumab, an anti–PD-1 antibody, has demonstrated significant survival benefit and a tolerable safety profile in patients with a variety of advanced/metastatic cancers. We have previously shown that popPK modeling supports a flat-dose regimen for tislelizumab across multiple oncologic indications, providing a more practical clinical dose regimen.

- What question did this study address?
  - This analysis provides an overview of the clinical pharmacology of tislelizumab, including pharmacokinetics, correlations with efficacy and safety, and immunogenicity properties, with a focus on patient race.

- What does this study add to our knowledge?
  - These analyses support the proposed flat-dose regimen of tislelizumab 200 mg intravenously once every 3 weeks and demonstrate that no dose modifications are needed based on race, as well as other intrinsic and extrinsic factors. E–R relationship analysis demonstrated that differences in exposure between Asian and White patients do not produce a clinically relevant impact on efficacy (OS and ORR) or safety. While numerical differences were observed in the clinical response and AE rates between treatment-emergent ADA-negative and ADA-positive patients of Asian and White race, these differences were not deemed to be clinically meaningful.

- How might this change clinical pharmacology or translational science?
  - As there were no clinically meaningful differences in the pharmacokinetics of tislelizumab, immunogenicity, and related efficacy/safety profiles between Asian and White patients in the studies included in this analysis, data generated from clinical studies of tislelizumab conducted primarily in Asia may be readily applied to White and other race populations.

1 | Introduction

Programmed cell death protein-1 (PD-1) and programmed death-ligand 1 (PD-L1) are immune checkpoint proteins that play a key role in regulating antitumor activity [1]. Binding of PD-1 to PD-L1 negatively regulates T-cell–mediated immune responses, resulting in immune evasion and T-cell exhaustion [2]. Anti–PD-1 and anti–PD-L1 monoclonal antibodies have been used successfully to treat a broad range of advanced solid tumors both as monotherapy or in combination with other treatments (e.g., other immunotherapies and chemotherapies) [2]. However, multiple mechanisms of resistance to PD-1/PD-L1 pathway blockade exist, including antibody clearance (CL) via antibody-dependent cellular phagocytosis (ADCP) through macrophage Fc gamma receptor (FcγR) binding [1, 3].

Tislelizumab (BGB-A317), a humanized immunoglobulin G4 monoclonal antibody that targets and binds to PD-1 with high affinity and specificity [3], was engineered to minimize FcγR1 binding on macrophages. This limits ADCP, which has been shown to compromise the antitumor activity of other anti–PD-1 monoclonal antibodies through activation of antibody-dependent, macrophage-mediated killing of T effector cells [3]. Tislelizumab is currently being investigated for the treatment of solid tumors and hematologic cancers as a monotherapy and combination therapy. After demonstrating robust antitumor efficacy and a tolerable safety profile in patients with advanced tumors, tislelizumab received National Medical Products Administration approval for 13 indications in China, as well as approvals in Europe, the United States, Australia, Brazil, Switzerland, the Republic of Korea, Singapore, Thailand, Israel, and the United Kingdom. With clinical trials of tislelizumab being conducted globally, it is important to understand whether tislelizumab has similar clinical effectiveness across different patient populations, especially those of different races.

Using population pharmacokinetic (popPK) simulations of data from patients with advanced solid tumors or classical Hodgkin lymphoma (cHL), we previously demonstrated that tislelizumab dose adjustment is not required for specific patient populations [4, 5]. In addition, there was no statistically significant correlation between the pharmacokinetic exposure of tislelizumab and objective response rate (ORR) or safety endpoints [5]. In this analysis, we provide an overview of the clinical pharmacology of tislelizumab, including pharmacokinetics, correlations with efficacy and safety, and immunogenicity properties, with a focus on patient race.

2 | Methods

Full details of the analysis dataset and characterization of the popPK modeling approach have previously been reported [4, 5]. Table S1 includes the study designs, patient populations, and analyses conducted [4].

All relevant institutional review boards/independent ethics committees reviewed the protocols and amendments and approved the studies, which were carried out in accordance with the International Conference on Harmonisation Good Clinical Practice Guideline, the principles of the Declaration of Helsinki, and local laws and regulations.

2.1 | Non-compartmental Analysis

A non-compartmental pharmacokinetic analysis was conducted to evaluate the pharmacokinetic profile of patients who were enrolled in BGB-A317-001 (data cutoff date: August 26, 2020) and BGB-A317-102 (data cutoff date: May 31, 2020).

2.2 | Population Pharmacokinetic Model Simulations

Using pooled data from 12 clinical studies, steady-state tislelizumab exposures were simulated using Bayesian post hoc individual pharmacokinetic parameters to evaluate the impact of intrinsic (i.e., race, age, renal impairment, hepatic impairment, and body weight) and extrinsic factors (i.e., food, smoking, and concomitant medications) on the pharmacokinetics of tislelizumab. Nonlinear mixed-effects modeling with first-order

conditional estimation with interaction in NONMEM, Version 7.3.0 (ICON Development Solutions, Ellicott City, Maryland, USA) was used.

2.3 | Exposure–Response (E–R) Relationships

Building on previously reported data [4, 5], E–R relationships were further evaluated in this analysis using data from patients who received tislelizumab 200 mg intravenously (IV) every 3 weeks (Q3W) in BGB-A317-302 (data cutoff date: December 1, 2020) and BGB-A317-303 (data cutoff date: August 10, 2020). Evaluable patients had received at least one adequately documented administration of tislelizumab and a corresponding efficacy or safety measurement. Model-predicted exposure metrics (maximum serum concentration at steady state [$C_{max,ss}$], minimum serum concentration at steady state [$C_{min,ss}$], average serum concentration at steady state [$C_{avg,ss}$], and average serum concentration of the first dose [$C_{avg,dose1}$]) were computed using the Bayesian post hoc pharmacokinetic parameters after tislelizumab administration (200 mg IV Q3W) for 30 weeks. E–R relationships for overall survival (OS) were explored by Kaplan–Meier estimates and analyzed by Cox proportional hazards modeling using $C_{avg,dose1}$, baseline patient characteristics (tumor size, Eastern Cooperative Oncology Group performance status [ECOG PS], albumin level, lactate dehydrogenase, aspartate aminotransferase [AST], alanine aminotransferase [ALT], bilirubin, estimated glomerular filtration rate, anti-drug antibody [ADA] status, age, weight, race, and sex), and tumor growth rate.

Two sensitivity analyses (tislelizumab arm alone, and tislelizumab and control [investigator-chosen chemotherapy] arms) were performed using OS data from BGB-A317-302 against exposure as a categorical variable (quartiles). E–R relationships for investigator-assessed ORR and safety endpoints were explored as the probability of response or adverse event (AE) incidence, respectively, versus tislelizumab exposure (bucketed by exposure quartiles). Logistic regression models using exposure as a continuous variable were developed by pooling patient data.

E–R relationships for safety endpoints—immune-mediated adverse events (imAEs), infusion-related reactions (IRRs), AEs of special interest (AESIs; imAEs plus IRRs), grade ≥ 3 AEs, and AEs leading to drug discontinuation or dose modification—were assessed using data from BGB-A317-302 and BGB-A317-303. Exposure–safety evaluable patients had at least one adequately documented administration of tislelizumab and corresponding post-dose safety data. The model-predicted exposure metrics ($C_{max,ss}$, $C_{min,ss}$, $C_{avg,ss}$, and $C_{avg,dose1}$) were computed using the Bayesian post hoc pharmacokinetic parameters as previously described.

2.4 | Immunogenicity

Immunogenicity was evaluated using data from BGB-A317-302 and BGB-A317-303. The presence of serum antibodies in response to treatment with tislelizumab was assessed using a validated conventional bridging assay. Neutralizing antibodies (NAbs) were assessed using a validated competitive PD-1 binding assay (LabCorp Covance, Shanghai, China). The immunogenicity assessment

schedule included predose samples at Cycles 1, 2, 5, 9, and 17, up to 1 year, and at the safety follow-up visit in general. Patients evaluable for immunogenicity assessment had a baseline ADA sample and at least one ADA sample taken after drug administration during the treatment or follow-up observation period.

3 | Results

3.1 | Non-compartmental Pharmacokinetic Analysis

Mean pharmacokinetic profiles in Cycles 1 and 4 (or 5) after tislelizumab IV dosing are presented in Figure 1a–c for BGB-A317-001 and Figure 1d for BGB-A317-102. In BGB-A317-001, which had a predominantly White population (87.2%, $n = 95/109$), tislelizumab exhibited a dose-proportional increase in exposure over 0.5 mg/kg to 10 mg/kg after the first dose administration (Table 1). Moderate interpatient variability was observed for both single and multiple dose phases. The coefficient of variation of pharmacokinetic parameters at the Cycle 1 dose ranged from 24.7% to 41.8% and 19.9% to 27.8% for the area under the serum concentration–time curve (AUC) during the dosing interval (AUC_{0-tau}) and C_{max}, respectively. The geometric means of AUC (95% CI) from time 0 to 21 days at Cycle 1 and AUC from time 0 to 21 days at Cycle 5 were 644.0 (513.0, 809.0; $n = 12$) and 825.0 (313.0, 2174.0; $n = 5$) μg*day/mL, respectively. The apparent terminal half-lives estimated in Cycles 1 and 5 were 15.9 and 14.9 days, respectively. The accumulation indices were 1.2 and 1.6, determined by the ratio of steady state and first dose of C_{max} and AUC_{0-tau}, respectively.

In BGB-A317-102, which enrolled Chinese patients only, the geometric mean of AUC_{0-tau} (95% CI) was 582.0 (516.0, 657.0) μg*-day/mL ($n = 20$) at Cycle 1 and 1073.0 (881.0, 1307.0) μg*day/mL ($n = 12$) at Cycle 5 (Table 2). The accumulation index (geometric mean [90% CI]), determined by pharmacokinetic exposures (ratio of steady-state to first dose AUC_{0-tau}, C_{max}, and observed concentration before the next dose [C_{trough}]), ranged between 1.9 (1.6, 2.2) and 2.1 (1.7, 2.6). Tislelizumab clearance (CL) and CL at steady-state values (geometric mean [95% confidence interval (CI)]) at Cycles 1 and 5 were 0.2 (0.2, 0.3) and 0.2 (0.2, 0.3) L/day, respectively.

3.2 | PopPK Model Simulations

The popPK model included 14,473 measurable tislelizumab concentrations from 2596 patients with advanced solid tumors or cHL across the 12 clinical studies identified in Table S1. Based on covariate analysis findings and subsequent model simulations, dose adjustments were not warranted.

3.3 | Evaluation of Intrinsic Factors on the Pharmacokinetics of Tislelizumab

3.3.1 | Race

Simulations of the Asian patient population from the 12 studies indicated that geometric mean exposures (AUC_{ss}, $C_{max,ss}$, and $C_{min,ss}$) were approximately 12% to 21% higher than those
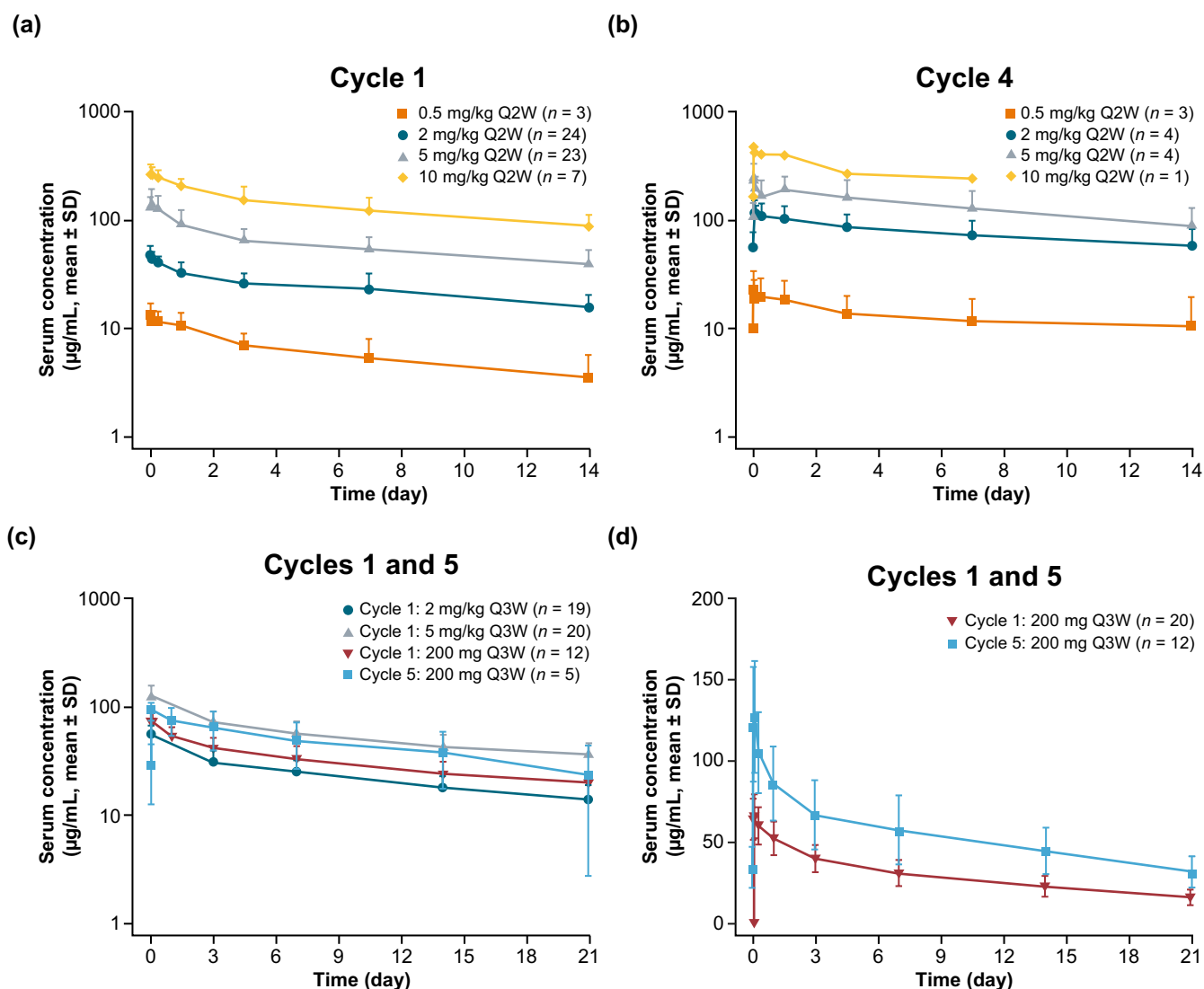
FIGURE 1 | Mean (AM ± SD) serum concentration of tislelizumab (single and multiple IV doses) during Cycle 1 (a, c), Cycle 4 (b), and Cycle 5 (c) in the BGB-A317-001 study, and during Cycle 1 and Cycle 5 (d) following 200 mg IV Q3W dosing in the BGB-A317-102 study. The lower limit of quantitation = 0.4 µg/mL. AM, arithmetic mean; IV, intravenous; Q2W, once every 2 weeks; Q3W, once every 3 weeks; SD, standard deviation.

of White patients (Table 3). However, the overall range of tislelizumab exposure at 200 mg Q3W largely overlapped between both groups (Figure S1). The differences by race were also small relative to the overall variability of exposures (Table 3), potentially due to body weight and other confounding covariates, and were not considered clinically relevant.

3.3.2 | Age

Although baseline age was identified as a covariate on the central volume of distribution (V_c) of tislelizumab, the estimate of V_c at the 10th and 90th percentiles of age distribution (45 and 71 years; Table S2) was within 3% of the typical estimate. The predicted steady-state exposures after 200 mg Q3W dosing for patients stratified by age groups are presented in Figure S2. In addition, the geometric mean simulated exposures (AUC_{ss}, $C_{max,ss}$, and $C_{min,ss}$) across all age ranges (<65 years, 65–75 years, ≥75 years) were consistent (Table S2). Therefore, the age effect on tislelizumab

pharmacokinetics was not clinically meaningful, and age-based dose adjustments are not needed for tislelizumab.

3.3.3 | Body Weight

Although baseline body weight was identified as a covariate on the CL and V_c of tislelizumab, the differences between the 10th and 90th percentiles of body weight distribution were small relative to the overall variability in exposures and were not considered clinically relevant. To further explore the impact of flat-dose tislelizumab on pharmacokinetic variability, the exposure range with the clinically recommended dose of 200 mg IV Q3W was compared with a hypothetical scenario of body weight-based dosing to assess the impact on the mean and variability in exposure. A 3 mg/kg dose was chosen for this hypothetical scenario as it corresponds to a 200 mg dose in a 65 kg patient (median weight in the popPK dataset). The means and variability in predicted steady-state exposures after 200 mg or

TABLE 1 | Summary of the pharmacokinetic parameters (non-compartmental analysis) of tislelizumab following single and multiple IV doses in the BGB-A317-001 study.

Dose level	Cycle 1, GM (GCV%)				Cycle 4 or Cycle 5,[a] GM (GCV%)				Accumulation indices of C_{max} (90% CI) AUC_{0-tau} (90% CI)
	n	C_{max} (µg/mL)	AUC_{0-tau} (µg/mL*day)	$AUC_{0-\infty}$ (µg/mL*day)	n	C_{max} (µg/mL)	AUC_{0-tau} (µg/mL*day)	Apparent terminal $t_{1/2}$ (day)	
Dose escalation and schedule expansion									
0.5 mg/kg IV Q2W	3	13.2 (27.8)	80.3 (41.8)	130 (67.2)	3	21.1 (57.2)	157 (71.5)	8.72 (6.7)	1.6 (1.2, 2.1) 2.0 (1.5, 2.6)
2 mg/kg IV Q2W	24	46.8 (23.9)	337 (25.2)	654 (37.1)	4	120 (21.1)	1033 (42.8)	17.4 (36.6)	2.7 (2.1, 3.4) 3.1 (2.3, 4.2)
5 mg/kg IV Q2W	23	132 (26.5)	823 (32.2)	1531 (55.9)	4	231 (40.0)	1780 (53.2)	12.1 (30.1)	1.6 (1.3, 1.8) 1.9 (1.5, 2.5)
10 mg/kg IV Q2W	7	273 (19.9)	1867 (25.3)	3642 (31.0)	1	476 (NE)	3453 (NE)	8.09 (NE)	1.3 (NE, NE) 1.4 (NE, NE)
2 mg/kg IV Q3W	19	55.5 (22.1)	498 (24.9)	857 (40.3)	—	—	—	—	—
5 mg/kg IV Q3W	20	126 (24.4)	1186 (24.7)	2129 (39.8)	—	—	—	—	—
Flat dose									
200 mg IV Q3W	12	76.1 (18.2)	644.0 (37.1)	1075.0 (53.9)	5	89.5 (20.6)	825.0 (91.6)	14.9 (127.0)	1.2 (1.0,1.4) 1.6 (1.2, 2.1)

Note: Population: 109 patients; sex (male/female): 50/59; race (White/Asian/Other): 95/10/4; median age: 60 (range 19.0–80.0) years; median body weight: 74.6 (range 43.0–120.4) kg.

Abbreviations: $AUC_{0-\infty}$, area under the serum concentration–time curve from time 0 to infinity; AUC_{0-tau}, area under the serum concentration–time curve during the dosing interval; CI, confidence interval; C_{max}, maximum serum concentration; GCV, geometric coefficient of variation; GM, geometric mean; IV, intravenous; NE, not evaluable; Q2W, once every 2 weeks; Q3W, once every 3 weeks; $t_{1/2}$, half-life.

The tau is 14 days for Q2W and 21 days for Q3W; 28 days per cycle for Q2W or 21 days per cycle for Q3W.

[a]The tau is 14 days for Q2W and 21 days for Q3W; 28 days per cycle for Q2W or 21 days per cycle for Q3W.

TABLE 2 | Summary of the pharmacokinetic parameters (non-compartmental analysis) of tislelizumab following 200 mg IV Q3W dosing in the BGB-A317-102 study.

Pharmacokinetic parameters	Cycle 1		Cycle 5		Accumulation index	Pseudo within-patient
	n	GM (95% CI)	n	GM (95% CI)	GMR[a] (90% CI)	%CV[b]
$AUC_{0\text{-tau}}$ (µg/mL*day)	20	582.0 (516.0, 657.0)	12	1073.0 (881.0, 1307.0)	1.9 (1.6, 2.2)	22.1
C_{max} (µg/mL)	20	66.5 (60.5, 73.2)	12	126.0 (104.0, 153.0)	1.9 (1.7, 2.2)	16.1
C_{trough} (µg/mL)	15	15.0 (12.5, 18.1)	11	30.1 (24.5, 37.0)	2.1 (1.7, 2.6)	28.7
CL (L/day)	20	0.2 (0.2, 0.3)	—	—	—	—
CL_{ss} (L/day)	—	—	12	0.2 (0.2, 0.2)	—	—

Note: Population: 20 patients; sex (male/female): 16/4; race (Chinese): 20; age: 49.5 (range 22.0–73.0) years; body weight: 66.0 (range 42.5–84.0) kg. 0.73% (3/412) of samples were excluded from the summary due to aberrant sample collection information. The tau is 21 days.

Abbreviations: %CV, percent coefficient of variation; $AUC_{0\text{-tau}}$, area under the serum concentration–time curve during the dosing interval; CI, confidence interval; CL, clearance; CL_{ss}, clearance at steady state; C_{max}, maximum serum concentration; C_{trough}, observed concentration before the next dose; GM, geometric mean; GMR, geometric least-squares mean ratio; IV, intravenous; Q3W, once every 3 weeks.

[a]GMR was used to calculate the Cycle 5 to Cycle 1 ratio of GMs of $AUC_{0\text{-tau}}$, C_{max}, and C_{trough}.

[b]Pseudo within-patient %CV $= 100 \times \text{sqrt}((S_a^2 + S_b^2 - 2 \cdot S_{ab})/2)$, where S_a^2 and S_b^2 are the estimated variances on the log scale for the 2 days, and S_{ab} is the corresponding estimated covariance, each obtained from the linear mixed-effects model.

TABLE 3 | Geometric mean (%CV) of steady-state tislelizumab exposure and baseline characteristics by race.

Characteristics		Race (N = 2573)		
		White	Asian	Other
Number of patients, n (%)		528 (20.5)	1991 (77.4)[a]	54 (2.1)
AUC_{ss} (µg*day/mL)	GM (%CV)	1150 (32.9)	1328 (26.7)	1144 (34.7)
	% difference[b]	Reference	15.6	−0.5
$C_{max,ss}$ (µg/mL)	GM (%CV)	101 (25.4)	113 (20.9)	102 (26.4)
	% difference[b]	Reference	12.0	1.1
$C_{min,ss}$ (µg/mL)	GM (%CV)	35.4 (42.0)	42.9 (33.8)	35.0 (46.4)
	% difference[b]	Reference	21.1	−1.4
Body weight, kg, median (range)		72.4 (39.1–130.0)	63.0 (31.9–113.0)	67.9 (41.8–110.0)
Albumin, g/L, median (range)		39.0 (20.0–380.0)	41.8 (17.0–435.0)	38.5 (20.0–46.0)
Age, years, median (range)		64.0 (18.0–90.0)	59.0 (18.0–83.0)	62.0 (22.0–88.0)
Tumor size, mm, median (range)		71.0 (10.0–408.0)	61.0 (10.0–355.0)	74.0 (10.0–301.0)
Sex, n (%)	Male	323 (61.2)	1545 (77.6)	32 (59.3)
	Female	205 (38.8)	446 (22.4)	22 (40.7)
ADAs, n (%)	Negative	423 (81.7)	1658 (83.9)	41 (75.9)
	Positive	95 (18.3)	318 (16.1)	13 (24.1)

Abbreviations: %CV, percent coefficient of variation; ADA, anti-drug antibody; AUC_{ss}, area under the serum concentration–time curve at steady state; $C_{max,ss}$, maximum serum concentration at steady state; $C_{min,ss}$, minimum serum concentration at steady state; GM, geometric mean.

[a]The Asian patient population was comprised of 1769 Chinese and 94 Taiwanese patients, as well as 128 non-Chinese patients (21 Australian, 3 French, 2 New Zealander, 1 British).

[b]% difference from the GM simulated exposures of the White patients in the overall population.

3 mg/kg IV Q3W dosing (Figure S3) were nearly identical, supporting the selection of the 200 mg IV Q3W flat dose.

3.3.4 | Renal Impairment

The impact of renal function on tislelizumab pharmacokinetic exposure was based on data from patients with normal ($n = 1223$; creatinine CL [CL_{CR}] ≥ 90 mL/min), mild ($n = 1046$; $CL_{CR} = 60$–89 mL/min), moderate ($n = 320$; $CL_{CR} = 30$–59 mL/min), and severe ($n = 5$; $CL_{CR} = 15$–29 mL/min) renal impairment. Renal function was not identified as a significant covariate. Based on the model-predicted exposures, mild and moderate renal impairment did not appear to have a clinically relevant impact on the pharmacokinetic properties of tislelizumab (Figure S4). Dose adjustments are not needed for tislelizumab when administered to patients with mild to moderate renal impairment. The available data were not sufficient to draw definitive conclusions for patients with severe renal impairment ($n = 5$).

3.3.5 | Hepatic Impairment

The liver function laboratory tests (AST, ALT, or total bilirubin) were not found to be covariates on tislelizumab pharmacokinetic properties in the popPK analysis. Based on National Cancer Institute Organ Dysfunction Working Group criteria, patients were classified into normal hepatic function ($n = 2182$; bilirubin $\leq$ upper limit of normal [ULN] and AST $\leq$ ULN), mild hepatic impairment ($n = 396$; bilirubin $\leq$ ULN and AST > ULN, or bilirubin > 1 to $1.5 \times$ ULN and any AST), moderate hepatic impairment ($n = 12$; bilirubin > 1.5 to $3 \times$ ULN and any AST), and severe hepatic impairment ($n = 2$; bilirubin > $3 \times$ ULN and any AST) groups. Comparing popPK model-predicted exposures between different hepatic impairment groups, there was no clinically relevant effect of liver function on the pharmacokinetic properties of tislelizumab (Figure S5). The analysis indicates that dose adjustments are not needed for patients with mild or moderate hepatic impairment. Limited data are available in patients with severe hepatic impairment; therefore, it was not possible to draw a definitive conclusion on the need for dose adjustments in these patients.

3.3.6 | Immunogenicity

The geometric mean of simulated exposures (AUC_{ss}, $C_{max,ss}$, and $C_{min,ss}$) in ADA-positive patients was 10.1% to 20.5% lower compared with those of ADA-negative patients. These differences were relatively small compared to the overall variability of exposures and were not considered clinically relevant. Therefore, dose adjustments are not warranted for tislelizumab based on ADA status. The predicted steady-state exposures after 200 mg Q3W dosing stratified by ADA status are presented in Figure S6.

3.4 | Evaluation of Extrinsic Factors on the Pharmacokinetics of Tislelizumab

As tislelizumab is a monoclonal antibody administered IV, extrinsic factors (i.e., food, smoking, and concomitant medications) are not expected to affect its pharmacokinetic properties.

Therefore, the effect of extrinsic factors on tislelizumab's pharmacokinetic properties has not been evaluated in previous studies or as part of the popPK analysis conducted in this analysis.

3.5 | E–R Relationship

As no time-varying CL was observed for tislelizumab, exposure metrics derived after the first dose and at steady state were correlated, and the model-predicted $C_{avg,dose1}$ was used as an exposure metric in the exposure–efficacy analysis. In total, 254 and 236 patients from BGB-A317-302, and 532 and 498 patients from BGB-A317-303 had both efficacy and pharmacokinetic data included in the analysis of OS (the primary endpoint) and ORR (a key secondary endpoint), respectively.

In the intention-to-treat population in BGB-A317-302, longer OS was observed in the highest exposure quartile versus the lower three quartiles (Figure 2a). Cox regression analysis showed that albumin, tumor growth rate, and tislelizumab $C_{avg,dose1}$ were predictors for OS ($p < 0.01$) (Figure 2b). Sensitivity analyses identified albumin level, tumor growth rate, and the highest exposure quartile as predictors for OS (Figure 2c). However, the lack of a consistent OS trend by exposure quartiles, the confounding effects of baseline disease characteristics such as tumor size and serum albumin levels on OS and tislelizumab CL, and the imbalance in the distribution of these baseline characteristics across exposure quartiles suggested there was no true association of exposure with efficacy.

Similarly, in BGB-A317-303, longer OS was observed in the intention-to-treat population ($n = 532$) with higher third and fourth exposure quartiles versus the lower two quartiles (Figure 3a). Cox regression analysis showed that lactate dehydrogenase, albumin, and tumor growth rate were predictors for OS ($p < 0.01$) (Figure 3b). However, $C_{avg,dose1}$ was not a predictor, suggesting no significant E–R relationship for OS after accounting for these confounding prognostic factors. The E–R relationship for OS was similar between White and Asian patients (Figure 3c).

Between responders (patients who achieved an objective response) and nonresponders in both BGB-A317-302 and BGB-A317-303 (Table S3), the range of tislelizumab exposure values was similar (Figure 4). The mean $\pm$ standard deviation of the tislelizumab $C_{avg,dose1}$ was 30.3 ± 4.30 µg/mL and 28.6 ± 4.55 µg/mL in responders versus 29.0 ± 5.16 µg/mL and 28.9 ± 4.79 µg/mL in nonresponders in BGB-A317-302 and BGB-A317-303, respectively (Figure 4a,b). Although a slight trend was observed between $C_{avg,dose1}$ and probability of response (Figure 4c,d), logistic regression modeling showed that $C_{avg,dose1}$ was not a predictor for ORR ($p > 0.05$). Tislelizumab exposures were similar between responders and nonresponders for Asian, White, and Other patients in both BGB-A317-302 and BGB-A317-303 (Figure 4a,b). The E–R relationship for the probability of objective response was also similar between White and Asian patients (Figure 4e).

The exposure–safety analysis included 254 and 532 patients with both safety data and pharmacokinetic data (C_{max}) from BGB-A317-302 and BGB-A317-303, respectively (Tables S4 and S5). No consistent or clinically relevant E–R relationships were observed for imAEs, IRRs, grade ≥ 3 AEs, AEs leading to
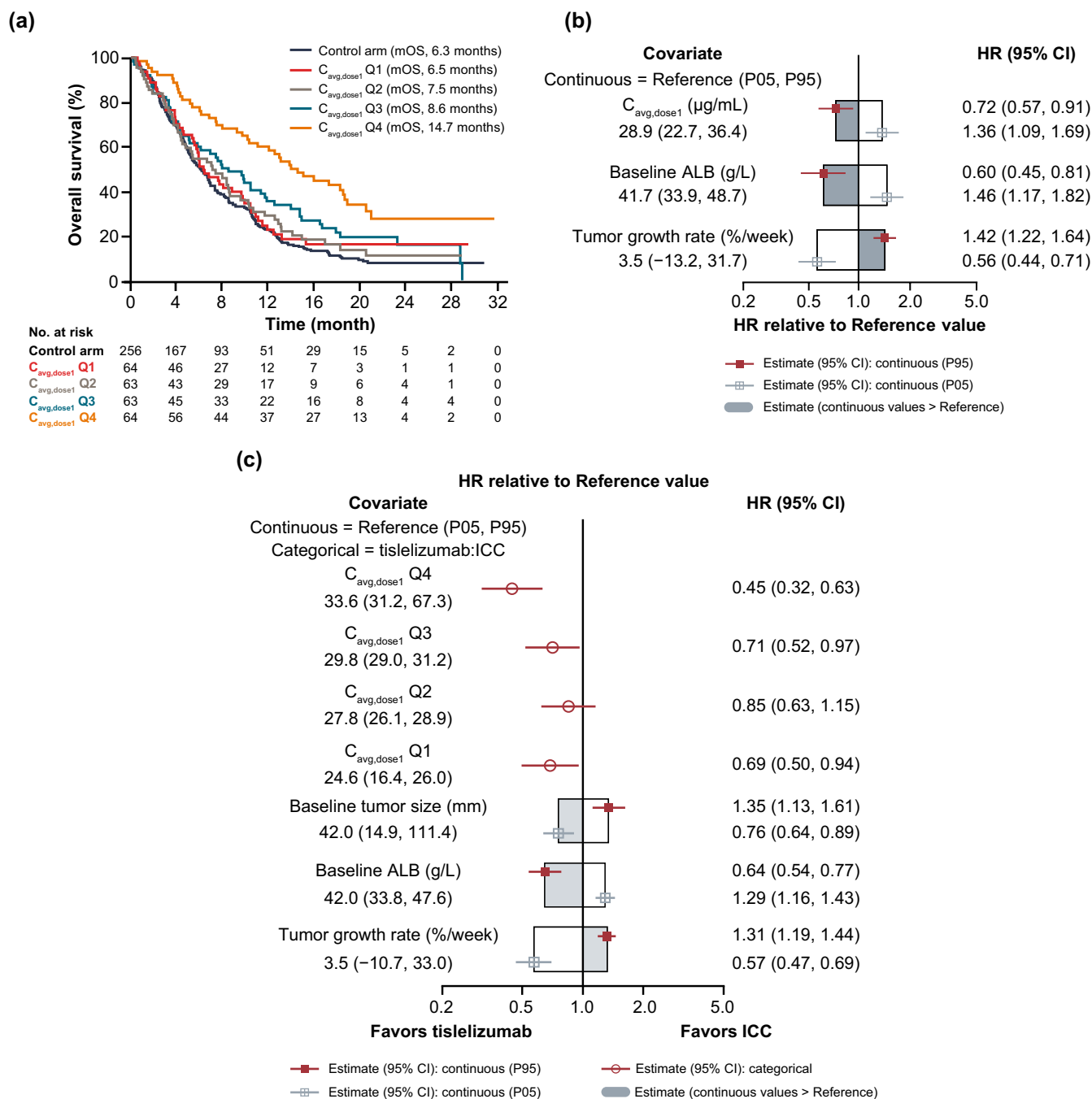
FIGURE 2 | Kaplan–Meier plot of OS stratified by $C_{avg,dose1}$ quartiles (a) and estimated effects of all predictor variables on the HR of OS (b) in tislelizumab-treated patients, and the estimated effects of prognostic factors and exposure quartiles on the HR of OS based on the combined dataset (c) in the BGB-A317-302 study. Panel a shows Kaplan–Meier curves stratified by quartiles of model-predicted $C_{avg,dose1}$ for the tislelizumab-treated group ($n = 254$) and ICC group ($n = 256$). Panel b shows the effect of each covariate on the HR of OS relative to a patient with reference values of covariates. The HR at the P05 and P95 are shown relative to the reference values. The shaded region of the box shows the estimate of the HR relative to the reference value when values of the continuous covariate are greater than the reference. Panel c shows the final OS model with all predictor variables for all patients in the BGB-A317-302 study. The graph describes the effect of each covariate on the HR of OS relative to a patient with reference values of covariates. The HR at the P05 and P95 are shown relative to the reference values. The shaded region of the box shows the estimate of the HR relative to the reference value when values of the continuous covariate are greater than the reference. ALB, albumin; $C_{avg,dose1}$, average serum concentration of the first dose; CI, confidence interval; HR, hazard ratio; ICC, investigator-chosen chemotherapy; mOS, median overall survival; OS, overall survival; P05, 5th percentile; P95, 95th percentile; Q1/Q2/Q3/Q4, concentration quartiles from lowest to highest.

dose modification, AESIs, or AEs leading to drug discontinuation within the tislelizumab 200 mg IV Q3W exposure range (Figures S7 and S8). Moreover, there were no clear or apparent differences observed in safety events between White and Asian patients in BGB-A317-302 or BGB-A317-303 (Tables S4 and S5). Due to the limited sample size, it was not possible to assess differences in the exposure–safety relationship for the "Other" race subgroup.
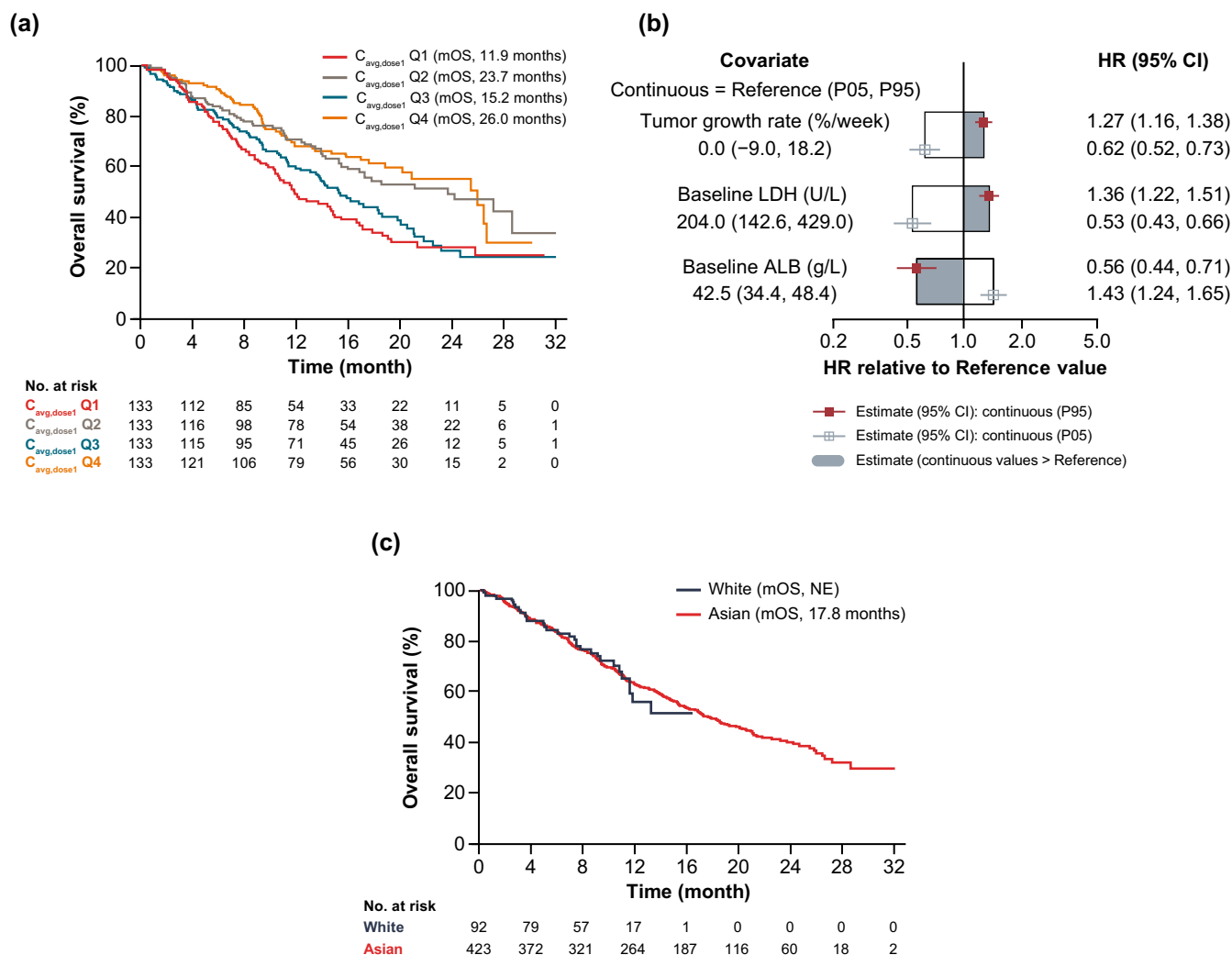
FIGURE 3 | Kaplan–Meier plot of OS stratified by $C_{avg,dose1}$ quartiles (a), the estimated effects of all predictor variables on the HR of OS (b), and the estimated effects of prognostic factors and exposure quartiles on the HR of OS based on the tislelizumab-treated overall population dataset (c) in the BGB-A317-303 study. Panel a shows Kaplan–Meier curves stratified by quartiles of model-predicted $C_{avg,dose1}$ for the tislelizumab-treated overall population ($n = 532$) in BGB-A317-303. Panel b shows the final OS model with all predictor variables for the tislelizumab-treated overall population ($n = 532$) in BGB-A317-303. The graph describes the effect of each covariate on the HR of OS relative to a patient with reference values of covariates. The HR at the P05 and P95 are shown relative to the reference values. The shaded region of the box shows the estimate of the HR relative to the reference value when values of the continuous covariate are greater than the reference. Panel c shows Kaplan–Meier curves stratified by race for the tislelizumab-treated overall population ($n = 532$) in BGB-A317-303. ALB, albumin; $C_{avg,dose1}$, average serum concentration of the first dose; CI, confidence interval; HR, hazard ratio; LDH, lactate dehydrogenase; mOS, median overall survival; NE, not estimable; OS, overall survival; P05, 5th percentile; P95, 95th percentile; Q1/Q2/Q3/Q4, concentration quartiles from lowest to highest.

3.6 | Incidence and popPK Analysis of Anti-Drug Antibodies

In BGB-A317-302, 14.5% of evaluable patients tested positive for treatment-emergent ADAs; NAbs were detected in 0.5% of patients (Table S6). Overall, 21.4% and 13.0% of evaluable White and Asian patients, respectively, tested positive for treatment-emergent ADAs; NAbs were detected in 0% of White patients and 0.6% of Asian patients. In BGB-A317-303, 20.5% of evaluable White patients tested positive for treatment-emergent ADAs compared with 14.3% of evaluable Asian patients; NAbs were detected in 1.2% and 0.2%, respectively.

While ADA status was a covariate, the flat E–R relationships, assessment of overall clinical response and safety events, and the presence of treatment-emergent ADAs did not impact tislelizumab's pharmacokinetic properties, efficacy, or safety to a clinically meaningful extent.

3.7 | Exploratory Analyses of the Relationship Between ADAs and Clinical Endpoints

In BGB-A317-302, comparable ORR (18.8% vs. 16.4%) and a numerically higher disease control rate (DCR; 56.3% vs. 51.3%)
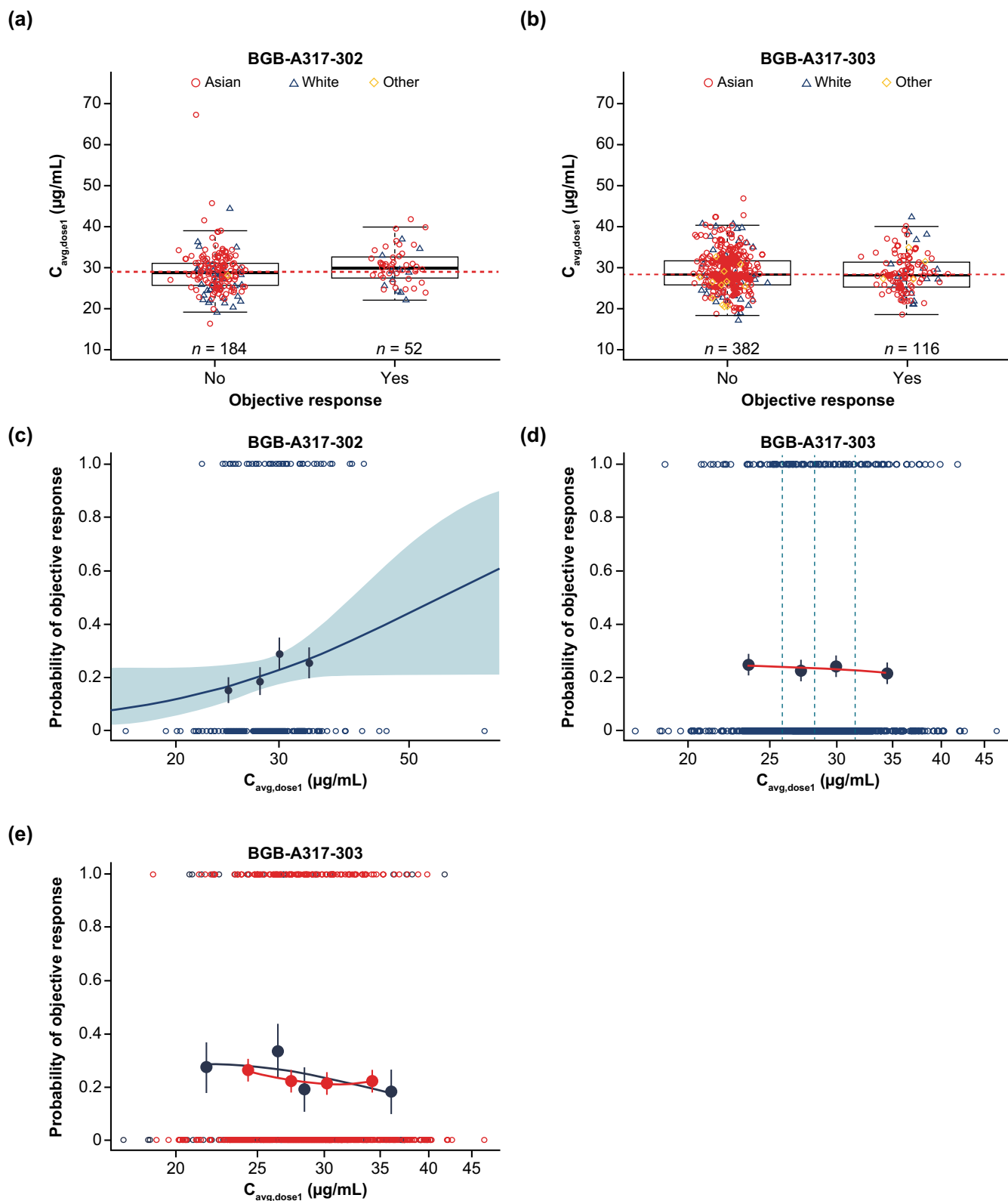
FIGURE 4 | Legend on next page.

were noted in the treatment-emergent ADA-positive versus ADA-negative groups, respectively; however, these differences were not considered clinically relevant (Table S7). ORR (21.7% vs. 16.2%) and DCR (52.2% vs. 50.0%) were numerically higher in Asian patients who were treatment-emergent ADA-positive

versus ADA-negative. ORR (11.1% vs. 18.2%) was numerically lower in White patients who were treatment-emergent ADA-positive versus ADA-negative; however, DCR was numerically higher (66.7% vs. 60.6%). These differences were not considered clinically meaningful (Table S8). Median OS was similar

FIGURE 4 | Relationship between tislelizumab exposure and ORR (a, b) and probability of objective response versus tislelizumab exposure (c, d) in patients with ESCC in the BGB-A317-302 study and patients with NSCLC in the BGB-A317-303 study, and by race in the BGB-A317-303 study (e). In panels a (BGB-A317-302) and b (BGB-A317-303), symbols are the model-predicted exposure metrics. The median is represented by the horizontal black line in the middle of each box. The lower and upper ends of the box plot represent the 25th and 75th percentile (the lower and upper quartiles, respectively). The bars extend to the most extreme data point, which is no more than $1.5 \times$ IQR from the box. The dashed red horizontal line represents the median value. In panel c (BGB-A317-302), the blue unfilled circles reflect the observed events. The filled navy solid circles are the observed probability of ORs and the error bars are the standard errors (calculated as sqrt $(P \times [1-P]/N)$) for quantiles (at $100 \times (1/4)$th percentiles) of exposures (plotted at the median value within each quantile). The blue line is the logistic regression model-predicted probability. The light blue shaded area is the 95% prediction interval based on 1000 bootstrap samples (probability: $0 =$ nonresponder; $1 =$ responder). In panel d (BGB-A317-303), the blue open circles reflect the observed events in tislelizumab-treated patients in BGB-A317-303. The navy solid circles are the observed probability of ORs and the error bars are the standard errors (calculated as sqrt $(P \times (1-P)/N)$), where P is the probability of OR and N is the number of patients in each quantile bin) for quartiles (25%, 50%, and 75%, blue vertical dotted lines) of exposures (plotted at the median value within each quartile). The red line is the smooth curve (LOESS) to show the relationship between two variables. In panel e (BGB-A317-303), the navy and red open circles reflect the observed events in tislelizumab-treated White ($n = 86$) and Asian ($n = 396$) patients, respectively. The navy and red solid circles are the observed probability of ORs and the error bars are the standard errors (calculated as sqrt $(P \times (1-P)/N)$) for White and Asian patients, respectively, where P is the probability of OR and N is the number of patients in each quantile bin) for quartiles of exposures (plotted at the median value within each quartile). The lines are smooth curves (LOESS) to show the relationship between two variables. $C_{avg,dose1}$, average serum concentration of the first dose; ESCC, esophageal squamous cell carcinoma; IQR, interquartile range; LOESS, locally estimated scatterplot smoothing; NSCLC, non-small cell lung cancer; OR, odds ratio; ORR, objective response rate; sqrt, square root.

between treatment-emergent ADA-positive ($n = 32$) and ADA-negative ($n = 189$) patients (10.0 vs. 10.3 months; hazard ratio [HR]: 1.05 [95% CI: 0.67, 1.65]; Figure S4a), and this was observed for both Asian and White patients (Figure S9b,c).

Comparable safety profiles were observed in BGB-A317-302, except that treatment-emergent ADA-negative patients had a lower rate of grade ≥ 3 AEs than ADA-positive patients (39.2% vs. 62.5%, respectively; Table S7). No hypersensitivity/IRR events developed after tislelizumab treatment. One grade ≥ 3 AE occurred on Day 22, and imAEs occurred on Days 22, 200, and 232. All AEs occurred before the NAb status turned positive on Day 251, indicating that NAb positivity was not related to these events. Among Asian patients, the rates of imAEs (21.7% vs. 21.4%) and AESIs (26.1% vs. 24.7%) were generally comparable between treatment-emergent ADA-positive versus ADA-negative patients, respectively, whereas the rates of grade ≥ 3 AEs (65.2% vs. 36.4%) and AEs leading to dose modification (26.1% vs. 20.8%) were numerically higher, and the rate of AEs leading to treatment discontinuation (8.7% vs. 18.2%) was numerically lower in ADA-positive patients than ADA-negative patients (Table S8). Among White patients, the rate of grade ≥ 3 AEs (55.6% vs. 51.5%) was comparable and the rate of AEs leading to treatment discontinuation (22.2% vs. 12.1%) was numerically higher in ADA-positive patients than in ADA-negative patients, respectively, whereas the rates of imAEs (11.1% vs. 15.2%), AESIs (11.1% vs. 15.2%), and AEs leading to dose modification (0% vs. 15.2%) were numerically lower.

In BGB-A317-303, numerically higher ORR (25.0% vs. 19.9%) and DCR (56.3% vs. 53.9%) were noted in the treatment-emergent ADA-positive versus ADA-negative groups, respectively; however, these differences were not considered clinically relevant (Table S9). ORR (27.6% vs. 19.2%), DCR (63.8% vs. 50.1%), and clinical benefit rate (56.9% vs. 43.3%) were numerically higher among Asian patients who were treatment-emergent ADA-positive versus ADA-negative, while DCR (35.3% vs. 74.2%) and clinical benefit rate (29.4% vs. 56.1%) were numerically lower in White patients who

were treatment-emergent ADA-positive versus ADA-negative; however, the differences were not considered clinically meaningful (Table S10). ORR was also similar among White patients who were treatment-emergent ADA-negative (24.2%) and ADA-positive (23.5%). Median OS was similar between treatment-emergent ADA-positive ($n = 80$) and ADA-negative ($n = 427$) patients (17.1 vs. 18.6 months; HR: 1.16 [95% CI: 0.84, 1.61]; Figure S10a), and this was observed for both Asian and White patients (Figure S10b,c).

In BGB-A317-303, treatment-emergent ADA-positive patients had numerically higher rates of grade ≥ 3 AEs (51.3% vs. 34.4%), imAEs (17.5% vs. 13.1%), AESIs (18.8% vs. 13.6%), AEs leading to treatment discontinuation (11.3% vs. 8.7%), and AEs leading to dose modification (31.3% vs. 20.6%) than ADA-negative patients (Table S9). Two patients developed NAb-positive ADAs (one on Day 21 and one during the safety follow-up period), of whom neither developed hypersensitivity, imAEs, or IRRs after tislelizumab treatment, and the onset of the first of other AEs occurred before the NAb became positive, indicating that NAb positivity was not related to these events. The rates of imAEs (19.0% vs. 14.9%), AESIs (19.0% vs. 15.2%), and AEs leading to treatment discontinuation (12.1% vs. 8.3%) were generally comparable between Asian patients who were ADA-positive and ADA-negative, whereas the rates of grade ≥ 3 AEs (48.3% vs. 35.8%) and AEs leading to dose modification (29.3% vs. 19.8%) were numerically higher in ADA-positive patients than ADA-negative patients (Table S10). Among White patients, the rates of grade ≥ 3 AEs (58.8% vs. 27.3%), imAEs (17.6% vs. 6.1%), AESIs (17.6% vs. 7.6%), and AEs leading to dose modification (35.3% vs. 24.2%) were numerically higher in ADA-positive patients than ADA-negative patients, whereas the rate of AEs leading to treatment discontinuation (5.9% vs. 10.6%) was numerically lower.

4 | Discussion

This analysis provides an overview of the clinical pharmacology of tislelizumab, including pharmacokinetics, correlations

with efficacy and safety, and immunogenicity properties, with a focus on patient race. Based on data from BGB-A317-001 and BGB-A317-102, in which the majority of patients were White and Asian, respectively, there was no difference in tislelizumab's pharmacokinetic parameters; therefore, dose adjustment of tislelizumab is not warranted based on race. The covariate analysis in the popPK model also showed no clinically meaningful effects of intrinsic factors, such as race, age, body weight, renal impairment, and hepatic impairment, on the pharmacokinetic properties of tislelizumab. Of note, geometric mean exposure was numerically higher in Asian versus White patients; however, the exposure differences, potentially attributable to body weight and other confounding covariates, were very small relative to the overall variability of exposures and were not considered clinically relevant.

No clinically meaningful E–R relationships for efficacy (ORR and OS) or safety (imAEs, IRRs, AEs of grade ≥ 3, AEs leading to dose modification, and AEs leading to drug discontinuation) were observed across any of the studies. Importantly, patient race (i.e., Asian vs. White/Other) had no clinically meaningful impact on exposure–efficacy relationships, and there were no clear or apparent differences observed in safety events, supporting the use of tislelizumab 200 mg IV Q3W in both populations.

Positive E–R relationships for OS have been reported for other monoclonal antibodies and immune checkpoint inhibitors, with a correlation between baseline CL and patient survival in oncology [6–10]. The severity of baseline disease conditions reflected by baseline albumin, tumor size, and ECOG PS, among other factors, has been known to be correlated with CL and, in turn, exposure. The severity of baseline disease status is also negatively associated with efficacy, thereby leading to an apparently positive E–R relationship. Thus, any E–R relationships are likely confounded by patient prognostic factors.

Overall, across all tislelizumab doses in the safety-evaluable studies, treatment-emergent ADAs and NAbs were observed in 16.5% and 0.6% of patients, respectively. The popPK analysis showed that, although ADA status was a covariate, the presence of treatment-emergent ADAs did not impact tislelizumab's pharmacokinetic properties, efficacy, or safety to a clinically meaningful extent. Moreover, the incidence of treatment-emergent ADAs was not associated with tumor type, patient sex, race, or any other covariates. While some differences were observed in the clinical response and AE rates between treatment-emergent ADA-negative and ADA-positive Asian and White patients in BGB-A317-303, these differences were not deemed to be clinically meaningful.

The 200 mg IV Q3W tislelizumab dose regimen was chosen because tislelizumab concentrations at this dose largely overlapped with those observed at the 2 mg/kg and 5 mg/kg IV Q3W doses [11]. The less frequent regimen of Q3W was selected based on the similarity in efficacy and safety events observed between the Q2W and Q3W regimens tested in the BGB-A317-001 study. Similar to other anti–PD-(L)1 agents, the flat dosing regimen of tislelizumab can be used in the treatment of solid tumors and cHL [12].

4.1 | Limitations

These data should be considered in the context of several limitations. First, the majority of patients in the pivotal studies were enrolled in China; however, no major differences were observed between patients of Asian and White race. Second, limited data were available for patients with severe hepatic function, which warrants further investigation. Third, a single dose level was evaluated in BGB-A317-302 and BGB-A317-303, which may have limited the ability to meaningfully assess E–R relationships due to potential imbalances in patient baseline characteristics.

5 | Conclusion

This analysis supports the proposed dosing regimen of tislelizumab at 200 mg IV Q3W and demonstrates that there were no differences in tislelizumab's pharmacokinetic or ADA characteristics among the patient populations investigated. Moreover, there was no clinically relevant E–R dependency for tislelizumab or impact of immunogenicity on efficacy (in terms of OS and ORR) or safety, and data were consistent across different populations including Asian and White patients. Therefore, data from the extensive clinical program of tislelizumab support the use of tislelizumab across broad patient populations with relevant tumor types.

Conflicts of Interest

Zhiyu Tang, Yanfei Yang, Ya Wan, Quting Zhang, Patrick Schnell, Ariadna Mendoza-Naranjo, Ramil Abdrashitov, William D. Hanley, and Nageshwar Budha are employees of and may own shares in BeiGene Ltd. Tian Yu, Chi-Yuan Wu, and Srikumar Sahasranaman were employees of BeiGene Ltd. at the time of the study and may own shares in BeiGene Ltd. Xianbin Tian and Ying Fei Li are employees of and may own shares in Novartis.

Data Availability Statement

BeOne Medicines (formerly known as BeiGene) voluntarily shares anonymous data on completed studies responsibly and provides qualified scientific and medical researchers access to anonymous data and supporting clinical trial documentation for clinical trials in dossiers for medicines and indications after submission and approval in the United States, China, and Europe. Clinical trials supporting subsequent local approvals, new indications, or combination products are eligible for sharing once corresponding regulatory approvals are achieved. BeOne Medicines shares data only when permitted by applicable data privacy

and security laws and regulations. In addition, data can only be shared when it is feasible to do so without compromising the privacy of study participants. Qualified researchers may submit data requests/research proposals for BeOne Medicines review and consideration through BeOne Medicines' Clinical Trial Webpage at https://www.beigene.com/our-science-and-medicines/our-clinical-trials/.

References

1. R. Dahan, E. Sega, J. Engelhardt, M. Selby, A. J. Korman, and J. V. Ravetch, "FcγRs Modulate the Anti-Tumor Activity of Antibodies Targeting the PD-1/PD-L1 Axis," *Cancer Cell* 28, no. 3 (2015): 285–295.

2. J. A. Seidel, A. Otsuka, and K. Kabashima, "Anti-PD-1 and Anti-CTLA-4 Therapies in Cancer: Mechanisms of Action, Efficacy, and Limitations," *Frontiers in Oncology* 8 (2018): 86.

3. T. Zhang, X. Song, L. Xu, et al., "The Binding of an Anti-PD-1 Antibody to FcγRI Has a Profound Impact on Its Biological Functions," *Cancer Immunology, Immunotherapy* 67, no. 7 (2018): 1079–1090.

4. N. Budha, C. Y. Wu, Z. Tang, et al., "Model-Based Population Pharmacokinetic Analysis of Tislelizumab in Patients With Advanced Tumors," *CPT: Pharmacometrics & Systems Pharmacology* 12, no. 1 (2023): 95–109.

5. T. Yu, X. Liu, C. Y. Wu, et al., "Clinical Dose Rationale of Tislelizumab in Patients With Solid or Hematological Advanced Tumors," *Clinical and Translational Science* 17, no. 3 (2024): e13769.

6. S. Agrawal, Y. Feng, A. Roy, G. Kollia, and B. Lestini, "Nivolumab Dose Selection: Challenges, Opportunities, and Lessons Learned for Cancer Immunotherapy," *Journal for Immunotherapy of Cancer* 4 (2016): 72.

7. P. Baverel, L. Roskos, M. Tatipalli, et al., "Exposure-Response Analysis of Overall Survival for Tremelimumab in Unresectable Malignant Mesothelioma: The Confounding Effect of Disease Status," *Clinical and Translational Science* 12, no. 5 (2019): 450–458.

8. Y. Feng, A. Roy, E. Masson, T. T. Chen, R. Humphrey, and J. S. Weber, "Exposure-Response Relationships of the Efficacy and Safety of Ipilimumab in Patients With Advanced Melanoma," *Clinical Cancer Research* 19, no. 14 (2013): 3977–3986.

9. C. Liu, J. Yu, H. Li, et al., "Association of Time-Varying Clearance of Nivolumab With Disease Dynamics and Its Implications on Exposure Response Analysis," *Clinical Pharmacology and Therapeutics* 101, no. 5 (2017): 657–666.

10. D. C. Turner, A. G. Kondic, K. M. Anderson, et al., "Pembrolizumab Exposure-Response Assessments Challenged by Association of Cancer Cachexia and Catabolic Clearance," *Clinical Cancer Research* 24, no. 23 (2018): 5841–5849.

11. J. Desai, S. Deva, J. S. Lee, et al., "Phase IA/IB Study of Single-Agent Tislelizumab, an Investigational Anti-PD-1 Antibody, in Solid Tumors," *Journal for Immunotherapy of Cancer* 8, no. 1 (2020): e000453.

12. M. Centanni, D. Moes, I. F. Troconiz, J. Ciccolini, and J. G. C. van Hasselt, "Clinical Pharmacokinetics and Pharmacodynamics of Immune Checkpoint Inhibitors," *Clinical Pharmacokinetics* 58, no. 7 (2019): 835–857.

Supporting Information

Additional supporting information can be found online in the Supporting Information section.